

Investigating snowpack volumes and icing dynamics in the moraine of an Arctic catchment using UAV/photogrammetry and LiDAR

É. Bernard¹, J.-M. Friedt², C. Marlin³, F. Tolle¹, M. Griselin¹, A. Prokop^{4,5}

¹ ThéMA/CNRS, University of Franche Comté, Besançon, France; *

² FEMTO-ST, University of Franche Comté, Besançon, France

³ GEOPS UMR 8148, CNRS - University of Paris Sud, France

⁴ Arctic Geology Department, The University Centre in Svalbard, UNIS, Norway

⁵ Snow Scan Research, Engineering, Education GmbH, Stadlauerstrasse 31, 1220 Vienna, Austria

January 25, 2017

Abstract

Means for assessing the contribution of the terminal moraine into the water budget of an Arctic glacier is investigated: on the one hand the terminal moraine represents a significant fraction (22%) of the catchment area of the glacier under investigation – Austre Lovénbreen, in the Brøgger peninsula, Spitsbergen – and on the other hand icings formation (or aufeis) each Winter illustrates the contribution of subglacial water flow. While over the glacier, with a smooth surface readily interpolated, the Winter and Summer mass balances are assessed with only a few sparsely distributed stakes, such an approach is not valid with the rough topography of the glacier moraine: high spatial resolution elevation models at different seasons are needed to estimate the volume of ice and snow accumulated during Winter in this part of the catchment basin and released in rivers during the melting season. Even if located at only 6 km from the Ny-Ålesund meteorological station, the moraine of Austre Lovénbreen catchment, can collect snow whose amount may differ from that given by station, due to drift snow and elevation-amount gradient, spatially and temporally variable. Surveying the terminal moraine by remote sensing methods is helpful for better quantifying the snow cover in proglacial moraine.

LiDAR – and in our case its terrestrial implementation – is currently the reference system for Digital Elevation Model generation: this highly specialized instrument provides utmost resolution with the drawback, when considering extended terminal moraine areas, of excessive shadows avoided by bringing the instrument to elevated measurement positions, a feat not necessarily achievable in given weather conditions or geographic settings. We consider the complementary use of commercial, off The Shelf (COTS) DJI Phantom3 Professional Unmanned Aerial Vehicle (UAV) for aerial photography acquisition, combined with Structure from Motion (SfM – using dedicated software as MicMac (French National Geographic Institute – IGN), Agisoft Photoscan and QGIS) analysis, for Digital Elevation Model (DEM) computation. DEM differences between datasets acquired in April (snow cover maximum and icings volume maximum) and September (snow cover minimum) yield a volume difference attributed either to snow cover or icing formation. Repeated measurements over a short period and moraine regions whose topography is known to be stable hint at an elevation resolution in the decimeter range, well below the icings and snow accumulation in the meter range. While the vegetation-free moraine provides ideal conditions for SfM – with lateral resolution down to 5 cm/pixel when flying at an altitude of 100 m – snow and river ice covered areas are challenging for the feature matching step needed for SfM initialization. We observe that under appropriate lighting conditions, most significantly avoiding the long shadows associated with a low-lying sun and overcast conditions, well resolved DEMs are acquired and generate a useful dataset.

*eric.bernard@univ-fcomte.fr

1 Problem statement

1.1 Snowpack response to climate shift

As shown by several dedicated works ([1] and [2]), Arctic is one of the most affected region in the world by current climate shift. It is thus a reliable indicator to quantify these changes through its hydro-glaciological dynamics ([3], [4] and [5]). In such dynamics, snow related processes are considered to be a key parameter ([6]) especially with a consideration for its extreme variability due to air temperature shifts and increased precipitation as well ([7]). Demonstrated effects of rain events on the snowpack ([8] and [9]) show the importance of carefully examining the resulting dynamics. It impacts, indeed, directly melting processes and proglacial hydrologic dynamics as well ([10] and [11]). Hence, assessing the hydrological budget of a glacier basin requires measuring the contribution of its 3 geographical areas:

- the glacier itself. Snowpack quantification is quite easy due to the homogeneous topography of the glacier's surface. Snow height is measured on each accumulation/ablation stake providing specific mass balance (i.e. maximum snow accumulation on the glacier), and interpolated on its surface.
- the surrounding slopes are assumed to be a significant provider of snow according to the increase of avalanche activity. Nevertheless, monitoring slopes is quite difficult, due to high instability, unless using remote methods of measurements such as laser scanning.
- the proglacial moraine, which is positioned as a transfer interface, shows dynamics which generates an increase of its geometry changes, both in quantity and frequency. The complex topography makes observation and measurement difficult although necessary.

This paper focuses on this third area, which is the main interface between the glacier and its outlets. The work presented here deals with the quantification of proglacial moraine snowpack and icings. The observed climatic trend is indeed remarkable not only through moraine morphological changes ([12] and [13]), but also in the changing snowpack dynamics and properties. This is directly linked to the increase of both temperatures and precipitations that have an immediate impacts on snowpack. Along with this, the actual processes of glacial retreat consequently release a significant proglacial moraine expansion ([14] and [15]). As a consequence, the moraine snowpack increases, modifying the water stock balance. Considering these points, it is then necessary to estimate, in the same way as on the glacier and the slopes, the water equivalent represented by the snowpack in the moraine.

Therefore, observing and quantifying these processes is a key point but remains tricky: slopes and moraine are challenging environments where the unstable brittle materials are unsuitable to distribute sensors, while the rough topography of the moraine prevents the use of interpolation ([16]). Indeed, the snow and icing distribution in the moraine exhibits heterogeneities, e.g. snow drift accumulation and channels filled with snow and/or ice, with scales of the same order of magnitude than the topography, typically in the meter range. Furthermore, the changing topography does not allow to process data on the same basis. In this investigation, we focus on the latter part of the budget: mapping snow and ice distribution in the moraine requires a high, sub-meter, spatial resolution in both lateral directions and decimeter resolution in the altitude measurement.

Hence, we consider flexible methods of data acquisition through Structure from Motion (SfM) digital image processing from pictures acquired from a Remotely Piloted unmanned Aircraft System (RPAS). This leads to the generation of high resolution Digital Elevation Models (DEMs) within short time frames, and differences of DEMs for estimating snow and icing distribution in the moraine. The underlying goal is to assess the use of combine SfM and UAV as an efficient workflow to map and quantify cryosphere dynamics into a proglacial moraine, in a context of fast climate induced morphologic changes.

In this paper, we present results from snowpack and icings quantification over Austre Lovénbreen, Svalbard, pro-glacial moraine. Repeated UAV surveys were conducted in Autumn 2015 and in Spring 2016, with coincident field-based observations and LiDAR acquisitions. This enables an innovative method to quantify solid water stock and snowpack dynamics in a deglaciating Arctic catchment.

1.2 Geographical settings

The Arctic glacial basin we consider in this investigation, Austre Lovénbreen, is located on the West coast of Svalbard on the Brøgger peninsula (79 °N). This case study consists in a small land-terminating valley and polythermal glacier in a 10.58 km² basin. Since the LIA (Little Ice Age),

Austre lovénbreen is increasingly exposing forefield sediments to processes of mobilization and redistribution. Its pro-glacial moraine has thus grown continuously, representing today nearly 25% of the whole basin, with direct consequences on snowpack distribution and melting processes.

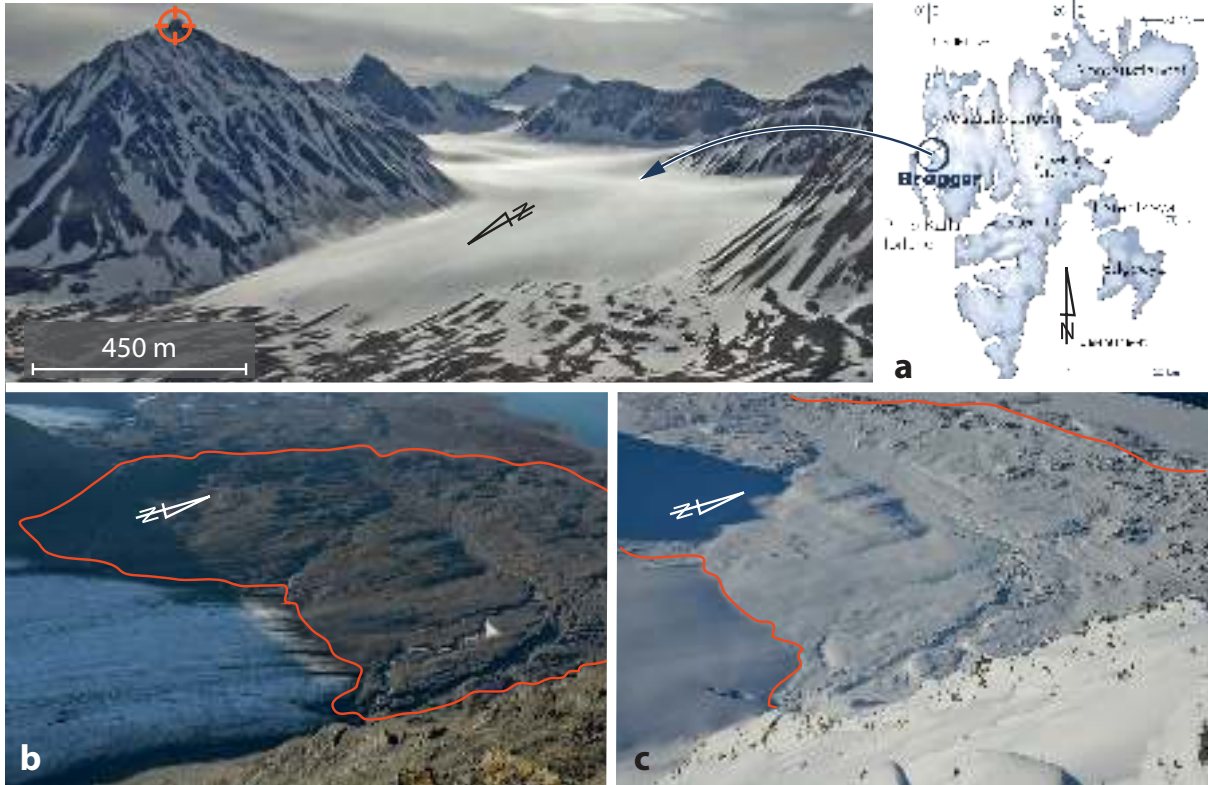


Figure 1: The fieldwork is located on the west coast of Spitsbergen (a). Proglacial moraine shown free of snow in Summer (b), and in Spring at its maximum snow accumulation (c). Photos (b) and (c) were taken from the Haavimbjället summit pointed on the panoramic view.

This highly dynamic environment, constitutes a snowpack base which is much more complex than the glacier topography itself.

Snowpack on the proglacial moraine is taking increasing importance compared to the snowpack on the glacier, changing the hydrological equation. As another consequence, quantification of this snowpack is quite tricky, and subject to a significant spatio-temporal variability. To assess photogrammetric methods of quantification, several representative “test areas” in the moraine were chosen in order to compare different data sets.

2 Research methods

2.1 Terrestrial laser scanning as a basis

Terrestrial measurement methods, whether photogrammetric or Light Detection and Ranging (LiDAR) topography mapping, are all plagued by excessive cast shadow effects from the grazing angle measurements. Throughout this investigation, the reference will be LiDAR scans acquired from Haavimbjället (783 m.a.s.l), a summit overlooking the glacier front as well as the whole pro-glacial moraine under investigation. Since 10 years, terrestrial LiDAR is extensively used for snow depth mapping and allows for accuracies in sub decimeter scale ([17], [18], [19] and [20]). The position chosen allows for limited shadow effects in the region exhibiting the strongest morphological variation, namely the outlet of a sub-glacial stream. LiDAR is however reluctantly considered for repeated mapping of the moraine area due to the challenge of bringing a cumbersome and fragile instrument in a physically demanding mountain environment. Nevertheless LiDAR, an active method, operates independently of lighting conditions and only requires clear atmosphere for light pulses to propagate

unhindered, a significant advantage in the Arctic environment characterized by a low lying Sun in the Fall period prior to the Arctic night and hence strong projected shadows challenging SfM processing (Fig. 2). All measurements were completed using a Riegl VZ-6000 laser scanner, operating at a wavelength of 1064 nm, selected for its strong reflectivity when illuminating snow and ice covered surfaces, with a measuring range of up to 6000 m, so the whole glacier catchment and moraine area could be covered by the single measurement position. Non-ground points were filtered using the wedge filtering approach ([21]). For referencing the two surfaces in respect to each other to calculate snow depths an iterative closest point algorithm was used ([22]). The accuracy of the LiDAR measurements were determined by reproducibility tests of the snow free areas and are in a range of 10 cm.

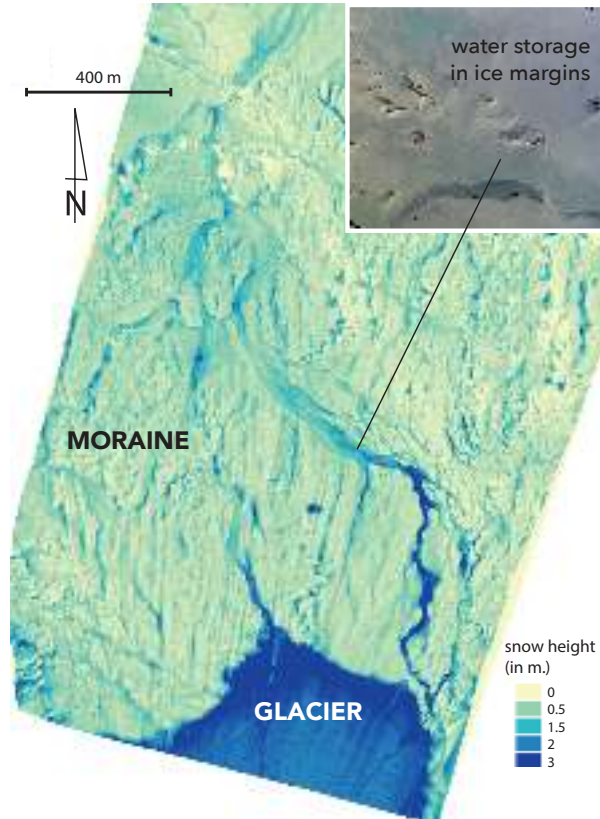


Figure 2: LiDAR map of elevation differences between Summer (August) and Winter (April) digital elevation models. Notice that the point cloud used to generate the DEM difference covered the whole moraine area in a single acquisition. The bottom dark blue area is the glacier exhibiting strong ablation during the Summer, while the light blue colored areas are the moraine with little elevation change since the 2016 Spring time exhibited low snow cover.

2.2 UAV data acquisition and processing

UAV consists in the best compromise for quality data acquisition, specifically when high spatio-temporal repeatability is needed ([23] and [24]). The images are acquired from a Commercial Off The Shelf (COTS) RPAS system selected for its ease of deployment – the aircraft and associated control systems fit in a lightweight backpack easily transported when walking in the moraine – while the low cost allows risking flight in challenging conditions: DJI Phantom 3 Professional and Advanced have demonstrated appropriate characteristics to the mapping task. The flight altitude is set to 100 to 110 m, providing a spatial resolution of 5×5 cm pixels when considering the optical system lens properties (94° angular coverage along the abscissa) and the sensor resolution (4000 pixel along the abscissa). The 15 minute autonomy at temperatures around 0° C and the horizontal speed of 10 m/s allow for covering a path length of about 9 km. The targeted 80% overlap between adjacent images, in the fast and slow raster scan axis, yields a covered area of about 700 to 1000 m \times 400 m. Hence,

most relevant parts of the 4 km² moraine are mapped with 10 flights lasting 15 minutes each, or less than half a day of activity. The significance of this aspect lies in the ability to process the dataset for generating orthophotos and digital elevation models under the assumption that no significant changes appear over such a short time lapse other than the cast shadow which prevents matching pictures of rough terrain imaged over time intervals of more than an hour. As an example of a result of such an acquisition, Fig. 3 compares an aerial image provided by the Norsk Polar Institute as a WMTS service ¹ acting as the background image over which we have added orthophotos generated from our flight datasets.



Figure 3: Comparison of an orthophoto available on the Norsk Polar Institute WMTS server acquired in 2010, and an orthophoto assembled from pictures acquired from an UAV in September 2015 as described in the text. The green line is a guide for the eye hinting at the 2015 glacier front position, emphasizing the glacier retreat and the sub-glacial stream, shown as a blue line on the left image, carving a new canyon in the newly deglaciated moraine area.

UAV flight sessions were prepared by analyzing the area of interest on a background satellite image in order to locate the flight limits. Real time video feedback allows for identifying features of interest on the ground, while the map displaying the GPS position of the UAV during flight over the background image hints at the covered area. The field of view of successive images, aimed at 80 to 60% overlap for SfM processing, is selected by manually triggering the on-board camera: considering an horizontal speed of 10 m/s, a flight altitude of 100 m and a field of view of 66° along the short picture axis (also the flight direction), each picture spans a length of 130 m, so that 80% overlap requires that the UAV has not flown more than 26 m along its path, hence requiring a picture to be taken once every 3 seconds at most. Thus, a 15 minute flight will generate about 300 pictures worth processing. Overlap in the long picture axis, from one track to another in a raster scanning flight path, is visually estimated on the map and is the strongest limit of the manual flight mode: while such an operating condition allows to adapt to ground features observed during flight – eg following a stream bed or valley of interest – it is less favorable to quantitative post-analysis over a wide area if overlap from one track to another is not sufficient. Such a case is observed on Fig. 3, in which the path of the UAV flying over the glacier and returning back towards the moraine was not sharp enough for the two-way paths to overlap over the glacier. SfM processing using MicMac (IGN, France – <https://github.com/micmacIGN>) was nevertheless able to handle the missing images and generated usable DEM and orthophoto with a hole of missing information where overlapping pictures were not available.

DEM difference requires sub-meter matching of successive acquisitions: the Coarse Acquisition L1 GPS receiver used to control the RPAS and tagging each acquired picture only provides ± 5 m accuracy (Fig. 4). The pointcloud, orthophoto and DEM are positioned with a weighted balance between photogrammetric processing and GPS camera positioning, with results depending on the practical implementation of the SfM algorithms and the weight given to the georeference tag associated with each picture. Our investigations focus on the comparison of the commercial Agisoft Photoscan software and the opensource MicMac available from the French National Geographic Institute (IGN). The same dataset was processed using similar workflow in both software, resulting in both cases in

¹http://geodata.npolar.no/arcgis/rest/services/Basisdata/NP_Ortofoto_Svalbard_WMTS_25833/MapServer/WMTS? or Toposvalbard at <http://toposvalbard.npolar.no/>

the same products, namely an orthophoto and a DEM: here we are not so much interested in the point cloud density, as was investigated earlier [25], than with the positioning accuracy.



Figure 4: Orthophoto of the area under consideration, with green lines indicating the shift between features found on the two orthophotos generated using MicMac and Agisoft Photoscan based on the same dataset of pictures annotated with the same GPS position found in the EXIF header. The typical green line length is 10 m.

While the general trend of the offset between the orthophotos generated by the two software is a north-east to south-west constant offset, some discrepancy remains even by adjusting this coarse offset. In order to reajust images and to improve measurement accuracy, “natural” GCPs were used such as easily identifiable erratic boulders. In the latter strategy, one DEM is selected as reference and the second DEM is moved to match features visible on the associated orthophoto. Considering that the LiDAR DEM is a reference, various SfM processing software yield different georeferencing accuracy when using solely the same camera shooting GPS position for positioning the DEM.

Indeed after translating one orthophoto along the vector defined by one of the green lines visible on Fig. 4, the remaining offset is in the 2.5 m range in the opposite corner than the one in which the reference line was selected. The resulting DEMs are either adjusted using ground based control points (GCPs) or matching features after acquisition by analyzing orthophotos.

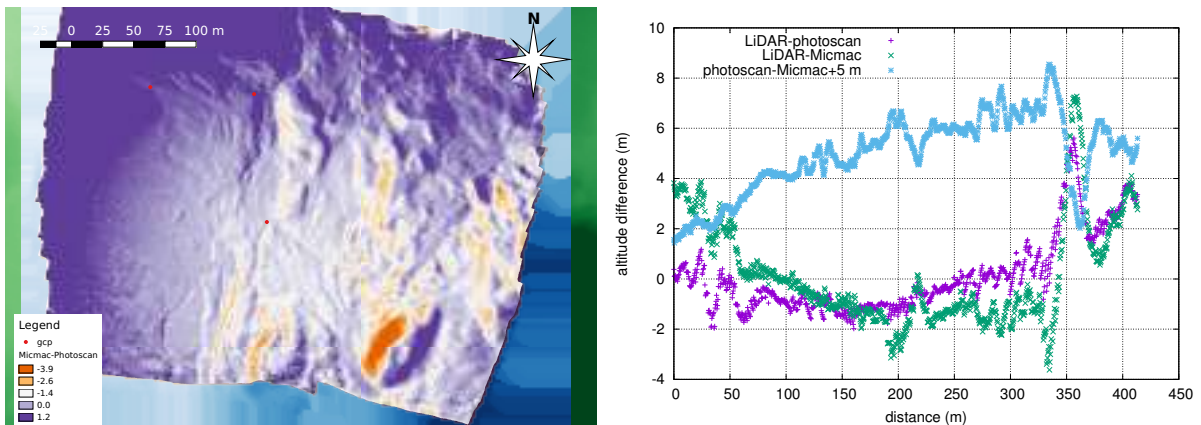


Figure 5: Left: map of the DEM difference. The positioning mismatch is obvious in the lower-right corner where a hill exhibits a positive height difference on the right and negative height difference on the left. Right: cross section of DEM differences between the airborne LiDAR dataset and two DEMs generated from photogrammetric processing of the same pictures with the same camera GPS coordinates provided in each picture EXIF header, using Agisoft Photoscan and MicMac.

Assuming an airborne LiDAR dataset recorded in August 2003 ([26]) provides utmost positioning accuracy, we assess the photogrammetry-generated DEM positioning accuracy with respect to this reference dataset. According to Arnold *et. al.* [27]), this LiDAR dataset consists in an acquisition collected at an altitude of 1600 m above sea level, giving a variable height above ground from 1600 m at the coast, to approximately 500–600 m above the peaks at the southern end of the catchment. All details of data acquisition are given by Arnold and other ([27]). Fig. 5 provides a cross-section comparing the elevation between the various DEMs. Computing standard deviations between abscissa 82 and 310 m on the elevation differences yield $\sigma_z = 0.6$ m between the airborne LiDAR and Photoscan generated DEM, $\sigma_z = 0.7$ m between airborne LiDAR and MicMac generated DEM, and $\sigma_z = 0.9$ m between the two photogrammetric-generated DEMs. The doming of the surfaces generated by photogrammetric processing, described in [28], is visible on the UAV-generated DEM subtracted to the LiDAR DEM, the latter not being affected by such lens modelling distortion effects. The effect is compensated for when subtracting two DEMs generated by independent photogrammetric processing software, hinting at both algorithms being identically affected by the erroneous lens modelling distortion effect.

3 Results and discussion

3.1 Estimating ice volume from DEM difference

Having analyzed the error bar on the DEM difference, and considering that the DEMs are matched using GCP identified on the reference orthophoto, we now consider the DEM difference for extracting snow depth and icing volume. Icings are punctual phenomenon, most of the time localized along rivers, where the ground topography constraints (generally sharp river channels) are the most important. The latter issue is thus most easily identified since icings form in well defined channels carved by the running water in Summer and, once filled with snow, create icings through snow transformation by the liquid water seeping from the glacier from Fall to Spring through Winter. This stratified ice formed from the freezing of successive outflows ([29]) appears at typical channel heights from 1 to 5 m which might not be fully filled by ice but hint at thicknesses well above the measurement uncertainty on the DEM difference. Indeed, the channels concentrating icing formations are well visible as shown in Fig. 6.

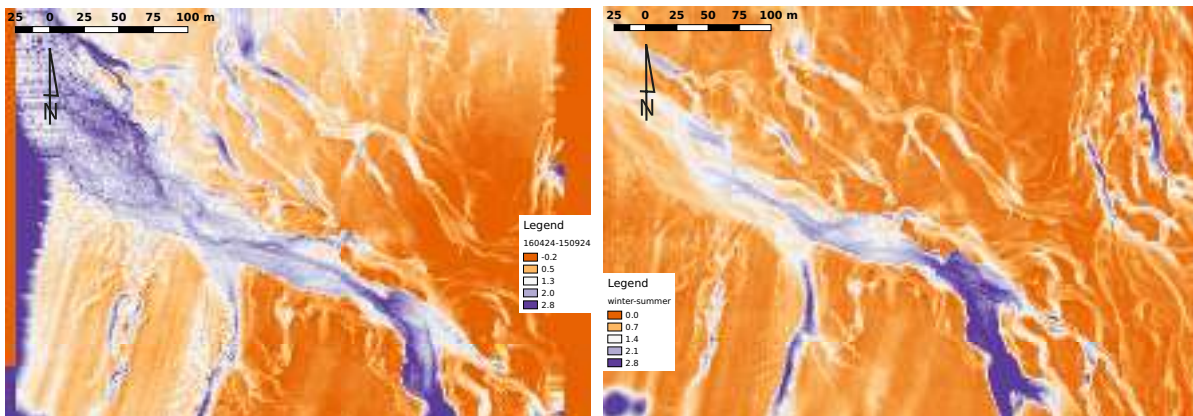


Figure 6: Left: difference of DEMs generated from SfM and adjusted through a translation for GCPs to match. The legend indicates the two dates at which the data were acquired, namely 24 April 2016 and 24 September 2015. Right: difference of DEMs generated by the LiDAR.

A core assumption when computing icing and snowpack volume is that the underlying moraine topography does not evolve between the two measurement sessions and that any elevation change is attributed to snow and ice accumulation and not to moraine mechanical erosion due to major flood induced by strong outflows generated by rain event(s). Such an assumption is met if the reference DEM is acquired at the end of the Summer season, when liquid precipitations have ended and the moraine remains frozen until the first snow fall. This assumption is usually met if the reference model of the snow-free moraine topography is acquired at the end of the hydrological season – beginning of October – although a sudden flood late in the season might require a later reference flight if the moraine topography is significantly affected. Throughout the following analysis, the hypothesis of a

given moraine topography during Autumn and Winter is met and all elevation changes are attributed to snow and ice accumulation.

3.2 Independent ice volume estimation

The volume of ice accumulated in the canyon concentrating flows from the glacier is estimated from difference of DEMs acquired at the minimum and maximum of the icings extent, integrating this difference over the canyon area. This phenomenon is indeed the most visible following the main canyon concentrating the most important water fluxes.

Using zonal statistics, and computing with the pixel size $0.09 \times 0.09 \text{ m}^2$, we obtain $1.1 \cdot 10^5 \pm 0.2 \cdot 10^5 \text{ m}^3$ of water stored in the ice margins.

Past hydrological measurements yield independent estimates in close agreement with this result. Indeed, [30] estimates a sub-glacial stream flow of $0.005 \text{ m}^3/\text{s}$: assuming this stream flow rate to be constant throughout the Winter lasting the 7 months from September to April, then the volume of water accumulating in the icings is $0.005 \text{ m}^3/\text{s} \times 86400 \text{ s/day} \times 181 \text{ days} \simeq 0.78 \cdot 10^5 \text{ m}^3$. Considering the rough assumption of constant flow, these two figures obtained from independent sources are in surprisingly good agreement, and provide an estimate of the sub-glacial stream contribution to the hydrological budget observed at the outlet of the moraine.

3.3 Snow distribution and quantification

The icings accumulating in the canyon carved by the sub-glacial stream are well analyzed with difference of DEMs integration since the elevation variations are well above the measurement resolution. We now wish to assess whether the snowpack distribution over the whole moraine can be analyzed similarly: the snowpack requires better elevation accuracy and is prone to misinterpretation of snow drift accumulation if the two DEMs are not well aligned.

Unlike the glacier itself and even less so the slopes, the moraine, due to its complex topography, is a challenging area for snowcover observation and monitoring. Snow free areas contrast with deep cornices accumulation likewise deep river channels filling. A few centimeters of snow are thus in opposition with, sometimes, more than 5 m snow accumulation. However, according to an accurate basis DEM, areas with clearly identifiable snowdrift are the easiest topographic configuration to assess snowpack height and volume. It gives the most important difference between maximum snow accumulation and snow free ground and makes it possible to check. But this required that data acquired gives sufficient contrast, which is not always the case with the high color homogeneity of snow.

Snowpack dynamics is a challenging measurement at the threshold of SfM accuracy. While the changing moraine topography might be erroneously attributed to snow accumulation, most significantly the strong topographic variation requires sub-meter lateral positioning of one DEM with respect to the reference DEM to avoid artifacts attributed to snowdrift accumulation on the slopes of the hills in the moraine. Such erroneous alignments are readily identified as positive accumulation on one side of the hill associated with negative height difference on the opposite slope (Fig. 5).

Climatic conditions of the considered 2015-2016 hydrological year were unfortunately not well suited for this demonstration. Indeed, although precipitation were abnormally high, most of them were liquid, making this year one of the worst of the last decade in terms of snow accumulation. The glacier snowpack was the second shallowest of the last 9 years recorded. The glacier snowpack measured in April 2016 was 491 mm.SWE (Snow Water Equivalent) while the past 9 year mean was 790 mm.SWE.

Consequently, we observed little accumulation in the moraine: the shallow snowpack provides, thus, especially poor conditions for this demonstration. Hence, we consider as a reference dataset the difference of LiDAR DEMs (Fig. 2) acquired at the end of April 2016 (theoretically to the maximum snowpack depth) and August 2016 (reference state with the lowest snow level in the moraine). Making the overall difference between the 2 LiDAR DEM available, accumulation areas appear clearly, specifically into the deepest canyons of the moraine. Moreover, considering the resolution and according to what was recently observed about proglacial moraine movement ([16]), it is quite difficult to attribute volume differences to snow accumulation or morainic materials. Short warm and rainy events are known to be responsible of significant morphological changes into the proglacial moraine. Thus, we can assume that part of the changed volume measured between April and October flight campaigns can be attributed to proglacial moraine geometry changes which occurred following the strong Summer melting outflows.

4 Conclusion

This work assesses the use of combined UAV and Structure from Motion methods for volume quantification in an Arctic environment. More specifically, this method is well adapted to analyze short event inducing significant topographical changes – sudden rain on snow events washing the snow-cover or heavy snow fall – as well as quantifying icing accumulation throughout the hydrological year. The orthophotos are well suited for quantifying snow and ice distribution in the moraine, as well as following detailed hydrological processes such as stream braiding or flow shift. However, quantifying height differences between the theoretical maximum snow accumulation and, at the opposite, the end of hydrological year when only few firn packs and icings remain, requires improvement on the positioning of DEMs, best addressed by better GCP use in the SfM process flow. The LiDAR process flow integrates GCPs as reflective target corner reflectors for matching point cloud positions, improving the accuracy of the DEM positioning enough for snowcover volume estimates to become relevant. The issue of snow density measurement for converting snowcover thicknesses to water equivalent quantities needed in a hydrological budget remains the same for all remote sensing techniques.

Snowcover thickness and icing water equivalent are hence measured in remote areas, but the most challenging part remains to process a huge quantity of data, and to obtain an accurate result over a large monitored surface (i.e. the whole moraine surface). Our basic assumption, when measuring after the last rainfall at the end of Fall as the Winter sets in (end of the hydrological year, set October 1st) for assessing the icing and snow cover volume, is that the underlying moraine topography no longer changes, and that all topographic modifications observed from LiDAR or SfM are due to snow and ice accumulation. On the opposite, during the melt season, both ice and snow melt as well as morphological changes are measured on DEM differences, and only by considering snow-free or covered areas, as observed on the orthophotos, can the nature of the elevation change be attributed to melting or morainic material displacement.

The flexibility of small COTS UAV and SfM are well suited in the specific study of short-term cryosphere processes. They can be highlighted at a high spatial resolution which could be compared to LiDAR measurements. Moreover, fast changes induced by climate shift can be recorded thanks to the possibility of easy monitoring repeatability given by a small COTS UAV.

Acknowledgements

We acknowledge financial support from the French National Research Agency (ANR) and Franche-Comté county for travel grants, IPEV for logistic support, and Photocoptère S.A.S for technical support on UAV maintenance and regulations. G. Rees has kindly provided the airborne LiDAR DEM of Midtre Lovénbreen, part of which also mapped the Austre Lovénbreen moraine. We also acknowledge Damien Roy for geomatic and data process support in ThéMA laboratory.

References

- [1] J Oerlemans. Extracting a climate signal from 169 glacier records. *Science (New York, N.Y.)*, 308(5722):675–7, 2005.
- [2] Jon Ove Hagen, Jack Kohler, Kjetil Melvold, and JanGunnar Winther. Glaciers in Svalbard: mass balance, runoff and freshwater flux. *Polar Research*, 22(2):145–159, dec 2003.
- [3] Ken Whitehead, Brian Moorman, and Pablo Wainstein. Measuring daily surface elevation and velocity variations across a polythermal arctic glacier using ground-based photogrammetry. *Journal of Glaciology*, 60(224):1208–1220, 2014.
- [4] Jon Ove Hagen, Trond Eiken, Jack Kohler, and Kjetil Melvold. Geometry changes on Svalbard glaciers: mass-balance or dynamic response? *Annals of Glaciology*, 42:255–261, aug 2005.
- [5] Regine Hock. Temperature index melt modelling in mountain areas. *Journal of Hydrology*, 282(1-4):104–115, nov 2003.
- [6] Andrew Philip Wright. *The Impact of Meltwater Refreezing on the Mass Balance of a High Arctic Glacier*. PhD thesis, Bristol, 2005.
- [7] Markus Eckerstorfer and Hanne H. Christiansen. The High Arctic Maritime Snow Climate in Central Svalbard. *Arctic, Antarctic, and Alpine Research*, 43(1):11–21, feb 2011.
- [8] Aga Nowak and Andy Hodson. Hydrological response of a High-Arctic catchment to changing climate over the past 35 years : a case study of Bayelva watershed , Svalbard. *Polar Research*, 1(1):1–16, 2013.

- [9] Johannes Schöber, K. Schneider, K. Helfricht, P. Schattan, S. Achleitner, F. Schöberl, and R. Kirnbauer. Snow cover characteristics in a glacierized catchment in the Tyrolean Alps - Improved spatially distributed modelling by usage of Lidar data. *Journal of Hydrology*, jan 2014.
- [10] M. Bavay, T. Grünewald, and M. Lehning. Response of snow cover and runoff to climate change in high Alpine catchments of Eastern Switzerland. *Advances in Water Resources*, 55:4–16, may 2013.
- [11] É. Bernard, J.M. Friedt, F. Tolle, M. Griselin, G. Martin, D. Laffly, and C. Marlin. Monitoring seasonal snow dynamics using ground based high resolution photography (Austre Lovénbreen, Svalbard, 79N). *ISPRS Journal of Photogrammetry and Remote Sensing*, 75:92–100, jan 2013.
- [12] Grzegorz Rachlewicz. Paraglacial Modifications of Glacial Sediments Over Millennial to Decadal Time-Scales in the High Arctic (Billefjorden, Central Spitsbergen, Svalbard). *Quaestiones Geographicae*, 29(3):59–67, 2010.
- [13] Samuel Wiesmann, Ladina Steiner, Milo Pozzi, and Claudio Bozzini. Reconstructing Historic Glacier States Based on Terrestrial Oblique Photographs. *AutoCarto 2012*, pages 1–14, 2012.
- [14] Valentina Radić, Andrew Bliss, a. Cody Beedlow, Regine Hock, Evan Miles, and J. Graham Cogley. Regional and global projections of twenty-first century glacier mass changes in response to climate scenarios from global climate models. *Climate Dynamics*, 42(1-2):37–58, apr 2013.
- [15] Ireneusz Sobota. Icings and their role as an important element of the cryosphere in High Arctic glacier forefields. *Bulletin of Geography, Physical Geography series*, 10(10):81–93, 2016.
- [16] É Bernard, J M Friedt, F Tolle, Ch Marlin, and M Griselin. Using a small COTS UAV to quantify moraine dynamics induced by climate shift in Arctic environments. *International Journal of Remote Sensing*, 0(0):1–15, 2016.
- [17] Alexander Prokop. Assessing the applicability of terrestrial laser scanning for spatial snow depth measurements. *Cold Regions Science and Technology*, 54(3):155–163, nov 2008.
- [18] Alexander Prokop, M. Schirmer, M. Rub, M. Lehning, and M. Stocker. A comparison of measurement methods: Terrestrial laser scanning, tachymetry and snow probing for the determination of the spatial snow-depth distribution on slopes. *Annals of Glaciology*, 49:210–216, 2008.
- [19] Jeffrey S. Deems, Thomas H. Painter, and David C. Finnegan. Lidar measurement of snow depth: A review. *Journal of Glaciology*, 59(215):467–479, 2013.
- [20] Alexander Prokop, Peter Schön, Florian Singer, Gaëtan Pulfer, Mohamed Naaim, Emmanuel Thibert, and Alvaro Soruco. Merging terrestrial laser scanning technology with photogrammetric and total station data for the determination of avalanche modeling parameters. *Cold Regions Science and Technology*, 110:223–230, 2015.
- [21] Helmut Panholzer and Alexander Prokop. Wedge-filtering of geomorphologic terrestrial laser scan data. *Sensors (Switzerland)*, 13(2):2579–2594, 2013.
- [22] a. Prokop and H Panholzer. Assessing the capability of terrestrial laser scanning for monitoring slow moving landslides. *Natural Hazards and Earth System Science*, 9(6):1921–1928, 2009.
- [23] M.J. Westoby, J. Brasington, N.F. Glasser, M.J. Hambrey, and J.M. Reynolds. Structure-from-Motion’ photogrammetry: A low-cost, effective tool for geoscience applications. *Geomorphology*, 179:300–314, dec 2012.
- [24] Arko Lucieer, Darren Turner, Diana H. King, and Sharon a. Robinson. Using an Unmanned Aerial Vehicle (UAV) to capture micro-topography of Antarctic moss beds. *International Journal of Applied Earth Observation and Geoinformation*, 27:53–62, apr 2014.
- [25] R. Niederheiser, M. Mokros, J. Lange, H. Petschko, G. Prasicek, and S.O. Elberink. Deriving 3D point clouds from terrestrial photographs – comparison of different sensors and software. In *The International Archives of the Photogrammetry, Remote Sensing and Spatial Information Sciences*, volume XLI-B5, XXIII ISPRS Congress, Prague, Czech Republic, 2016.
- [26] WG Rees and NS Arnold. Mass balance and dynamics of a valley glacier measured by high-resolution LiDAR. *Polar Record*, 43(227), 2007.
- [27] N. S. Arnold, W. G. Rees, B. J. Devereux, and G. S. Amable. Evaluating the potential of high-resolution airborne LiDAR data in glaciology. *International Journal of Remote Sensing*, 27(6):1233–1251, 2006.

- [28] Mike R. James and Stuart Robson. Mitigating systematic error in topographic models derived from UAV and ground-based image networks. *Earth Surface processes and landforms*, 39:1413–1420, 2014.
- [29] E BukowskaJania and Joanna Szafraniec. Distribution and morphometric characteristics of icing fields in Svalbard. *Polar Research*, 24:41–53, 2005.
- [30] M. Griselin. Les marges glacées du Loven Est, Spitsberg : un milieu original lié aux écoulements sous-glaciaires. *Revue de géographie alpine*, 73(4):389–410, 1985.